Journal of Alloys and Compounds 502 (2010) 346–350

Contents lists available at ScienceDirect

Journal of Alloys and Compounds

journal homepage: www.elsevier.com/locate/jallcom

Improvement of corrosion resistance and magnetic properties of Nd–Fe–B sintered magnets by $Al_{85}Cu_{15}$ intergranular addition

J.J. Ni[a,b], T.Y. Ma[a], X.G. Cui[a], Y.R. Wu[a], M. Yan[a,*]

[a] Department of Material Science and Engineering, State Key Laboratory of Silicon Materials, Zhejiang University, No. 38 Zheda Road, Hangzhou 310027, China
[b] College of Material Science and Engineering, Liaocheng University, Liaocheng 252059, China

ARTICLE INFO

Article history:
Received 7 December 2009
Received in revised form 30 March 2010
Accepted 2 April 2010
Available online 10 April 2010

PACS:
75.50.Bb
75.50.Ww
75.30.Gw

Keywords:
Nd–Fe–B sintered magnets
$Al_{85}Cu_{15}$ powders
Corrosion resistance
Magnetic properties

ABSTRACT

To improve the corrosion resistance and magnetic properties, $Al_{85}Cu_{15}$ (at.%) compound powders were added to $(Pr, Nd)_{14.8}Fe_{78.7}B_{6.5}$ sintered magnets as grain boundary modifiers. The corrosion resistance was found to be remarkably improved by small additions of $Al_{85}Cu_{15}$ powders. When 1.2 wt% $Al_{85}Cu_{15}$ was added, the corrosion rate of magnets in humid environments was reduced by two orders of magnitude. This is partly due to the stability enhancement of the (Pr, Nd)-rich intergranular phase by Cu and Al. In addition, the occurrence of the Cu-rich phase ($(Pr, Nd)_{22}Fe_{56}Cu_{10}Al_2O_{10}$), whose open-circuit potential is higher than the (Pr, Nd)-rich intergranular phase, may be another reason for the improvement of the corrosion resistance. Furthermore, the magnetic properties of $(Pr, Nd)_{14.8}Fe_{78.7}B_{6.5}$ were also improved by adding 0.3–1.2 wt% $Al_{85}Cu_{15}$. Optimum addition amount was 0.6 wt%. The improvement of the magnetic properties may be related to the microstructural modification and the increase of magnet density.
© 2010 Elsevier B.V. All rights reserved.

1. Introduction

Due to the outstanding magnetic properties, Nd–Fe–B sintered magnets have been used in various fields, like voice coil motors (VCM) for hard disk drives (HDD), medical instruments, automotive applications, industrial motors and generators, etc. However, the applications are limited by their poor corrosion resistance [1–3], which is related to the existence of multiple phases in the microstructure. The most important ferromagnetic phase present in Nd–Fe–B sintered magnets is $Nd_2Fe_{14}B$ matrix phase, which is basically surrounded by the Nd-rich intergranular phase. The Nd-rich phase is very active and corrodes preferentially [4,5], resulting in the intergranular corrosion of Nd–Fe–B sintered magnets. Therefore, to modify the intergranular phase is an important approach to improve the corrosion resistance of magnets.

According to Tomashov' theory on the alloy corrosion [6], the Nd-rich intergranular phase could be stabilized by additions of alloying elements with higher standard electrode potentials than neodymium. The standard electrode potentials for Cu^{2+}/Cu and Al^{3+}/Al are respectively 0.3419 and −1.632 V, much higher than Nd^{3+}/Nd (−2.431 V) [7]. Cu and Al are thus important candidates to enhance the corrosion resistance of Nd–Fe–B sintered magnets [8,9]. Generally, remarkable improvement of the corrosion resistance of magnets requires adding 1.7–2.0 at.% Cu [10,11] or 4–6 at.% Al [12,13] to the magnets prior to melting the alloy. Higher addition of Cu or Al may deteriorate the magnetic performance of Nd–Fe–B sintered magnets because of the magnetic dilution effect induced by the dissolution of Cu or Al in the $Nd_2Fe_{14}B$ phase [14]. So, to marginalize or avoid Cu and Al entering into the $Nd_2Fe_{14}B$ phase is a promising way to improve the corrosion resistance of magnets without sacrificing the magnetic properties.

Previous investigations have shown that the intergranular addition of Cu or Al could marginalize or avoid them entering into the $Nd_2Fe_{14}B$ phase [8,15]. Moreover, the combined additions of metal elements could be much more effective to improve the corrosion resistance of magnets [16]. So, possibly the intergranular addition of Cu and Al might improve the corrosion resistance of Nd–Fe–B sintered magnets without deteriorating their magnetic properties. In the present work, $Al_{85}Cu_{15}$ alloy powders were prepared and added to Nd–Fe–B sintered magnets. The effects of $Al_{85}Cu_{15}$ intergranular addition on the corrosion resistance and magnetic properties were investigated.

2. Experimental

The starting materials included Al, Cu and Fe with purities all above 99.9%, Pr–Nd containing 25 at.% Pr and Fe–B containing 20 at.% B. The $(Pr, Nd)_{14.8}Fe_{78.7}B_{6.5}$ (at.%)

* Corresponding author. Tel.: +86 571 87952730; fax: +86 571 87952366.
E-mail address: mse_yanmi@zju.edu.cn (M. Yan).

0925-8388/$ – see front matter © 2010 Elsevier B.V. All rights reserved.
doi:10.1016/j.jallcom.2010.04.021

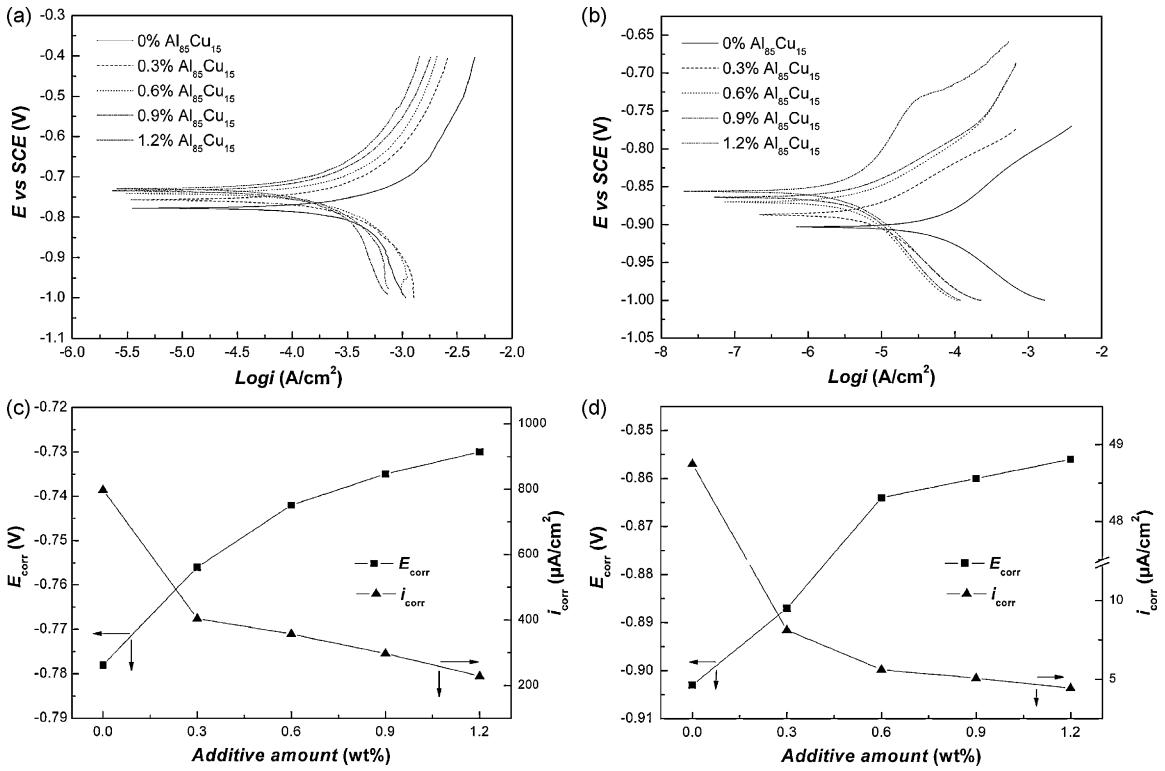

Fig. 1. Potentiokinetic polarization curves of magnets in Ar-purged (a) 0.049% H_2SO_4 and (b) 3.5% NaCl aqueous solutions; (c) and (d) are corrosion potentials and corrosion current densities corresponding to (a) and (b), respectively.

alloy ingot and $Al_{85}Cu_{15}$ (at.%) alloy ingot were respectively produced by vacuum induction melting. The $(Pr, Nd)_{14.8}Fe_{78.7}B_{6.5}$ ingot was first crushed and pulverized to less than 250 μm, and then were milled to fine powders with an average size of 4 μm through jet milling under the protection of nitrogen atmosphere. The $Al_{85}Cu_{15}$ ingot was crushed and pulverized to about 4 μm powders through ball milling (300 rpm) under argon atmosphere. The $(Pr, Nd)_{14.8}Fe_{78.7}B_{6.5}$ alloy powders were blended with 0.3–1.8 wt% $Al_{85}Cu_{15}$ powders through ball milling (60 rpm) for 1.5 h under the protection of nitrogen gas. After blending, the mixed powders were compacted at 6 MPa in a magnetic field of 1.6 T. Afterwards they were sintered for 2 h at 1090 °C followed by a two-step annealing treatment, which was performed for 2 h at 890 °C and subsequently for 3 h at 550 °C.

Magnetic properties were measured using an AMT-4 magnetic measurement device. Microstructures were observed under a filed emission scanning electron microscopy (FESEM SIRION-100) equipped with an energy dispersive X-ray spectroscopy (EDX). Magnet density was calculated using the Archimedes principle. Polarization curves were determined with a CHI604B electrochemistry analyzer. All experiments were performed in a standard three electrode cell consisting of Nd–Fe–B working electrode, saturated calomel reference electrode and Pt counter electrode. Experiments were conducted at 25 ± 0.1 °C in 0.049% H_2SO_4 (pH = 2) and 3.5% NaCl (pH = 7) aqueous solutions, which were purged with Ar gas for 1 h before the test. The Nd–Fe–B electrode was placed into the cell and the open-circuit potential was monitored for 15 min until it was stabilized. The potential scan rate was 2 mV/s along the direction from the negative potential to the positive one. Accelerated corrosion test was performed by placing cubic samples (10 mm × 10 mm × 10 mm) in 120 °C, 2 bar and 100% relative humid atmosphere for different times. The samples were ground with SiC paper (grade 320-1000) and then polished using diamond paste (1 μm) before corrosion test. After corrosion test, all corrosion products were removed from the magnet surfaces. The losses in mass were performed by weighing test samples before and after exposure using a microbalance with an accuracy of 0.1 mg and noted as mass loss related to the surface (mg/cm^2).

3. Results and discussion

3.1. Corrosion resistance

The potentiokinetic polarization curves for the tested magnets in 0.049% H_2SO_4 and 3.5% NaCl solutions are presented in Fig. 1a and b, respectively. Their corresponding corrosion potential E_{corr} and corrosion current density i_{corr} were obtained from the polarization curves by the Tafel slope extrapolation method [8] and respectively illustrated in Fig. 1c and d. For 0.049% H_2SO_4 and 3.5% NaCl solutions, at potentials a little more positive than E_{corr}, addition of $Al_{85}Cu_{15} \geq 0.3$ wt% in magnets moves the anodic curves towards smaller current densities. This indicates that the anodic process is inhibited by $Al_{85}Cu_{15}$ addition. With the increase of $Al_{85}Cu_{15}$ addition amount, E_{corr} becomes more positive and i_{corr} gets lower. For samples with $Al_{85}Cu_{15}$ addition from 0 to 0.6 and 1.2 wt%, in 0.049% H_2SO_4 solution E_{corr} increases from −0.778 to −0.742 and −0.731 V, respectively, but i_{corr} decreases from 798.3 to 357.7 and 228.6 μA/cm^2 accordingly. In 3.5% NaCl solution E_{corr} increases from −0.903 to −0.864 and −0.856 V, while i_{corr} decreases from 48.8 to 5.6 and 4.4 μA/cm^2, respectively. Results demonstrate that $Al_{85}Cu_{15}$ intergranular addition can improve the corrosion resistance of magnets in saline and weak acidic electrolytes. Higher additions of $Al_{85}Cu_{15}$ are beneficial to enhance the corrosion resistance.

Fig. 2 corresponds to the mass loss of magnets, as a measuring quantity for the determination of the corrosion rate in humid environments. As can be seen, the mass loss increases with exposure time, since the corrosion occurs only in the intergranular regions and those regions grow during the exposure [17]. For the $Al_{85}Cu_{15}$-free magnets, the mass loss can obviously be observed after 24 h. Up to 96 h, the mass loss reaches 114.9 mg/cm^2. However, the $Al_{85}Cu_{15}$-added magnets have no obvious mass loss before 72 h. Over 72 h, only a slightly increasing mass loss is observed. At 96 h, higher additions of $Al_{85}Cu_{15}$ decrease the mass losses of magnets. For the magnet with 1.2% $Al_{85}Cu_{15}$, the mass loss is 4.2 mg/cm^2, which has been decreased by two orders of magnitude in comparison with the $Al_{85}Cu_{15}$-free magnet. Results show that small additions of $Al_{85}Cu_{15}$ can also remarkably improve the corrosion resistance of Nd–Fe–B sintered magnets in humid environments.

EDX analysis showed that Cu and Al primarily distribute along the grain boundaries, which is consistent with our previous investigation [8]. Fig. 3a shows the SEM back-scattered image of the

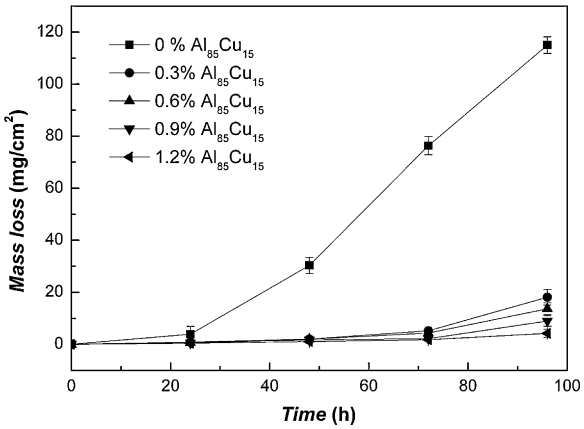

Fig. 2. Mass loss of magnets measured in 120 °C, 2 bar and 100% relative humidity atmosphere for different times. The error bar represents the standard deviation obtained from 5 samples.

magnet with 1.2 wt% $Al_{85}Cu_{15}$. In addition to the (Pr, Nd)-rich and (Pr, Nd)$_2$Fe$_{14}$B phases, Cu-rich phase was also detected. Similarly, the Cu-rich phase was found in other samples with different amounts of $Al_{85}Cu_{15}$. As shown in Fig. 3b, the compositions of the Cu-rich phase are approximately 22 at.% (Pr, Nd), 56 at.% Fe, 10 at.% Cu, 2 at.% Al and 10 at.% O (neglecting B). The atomic ratio of (Pr, Nd) to (Fe, Cu, Al) is about 1:3. According to previous literature [18], the Cu-rich phase should be a RFe_3-type phase. In order to investigate the Cu-rich phase effect on the corrosion resistance of magnets, alloys with compositions of (Pr, Nd)$_{22}$Fe$_{56}$Cu$_{10}$Al$_2$O$_{10}$ (Cu-rich phase), (Pr, Nd)$_{80}$Fe$_{20}$ ((Pr, Nd)-rich

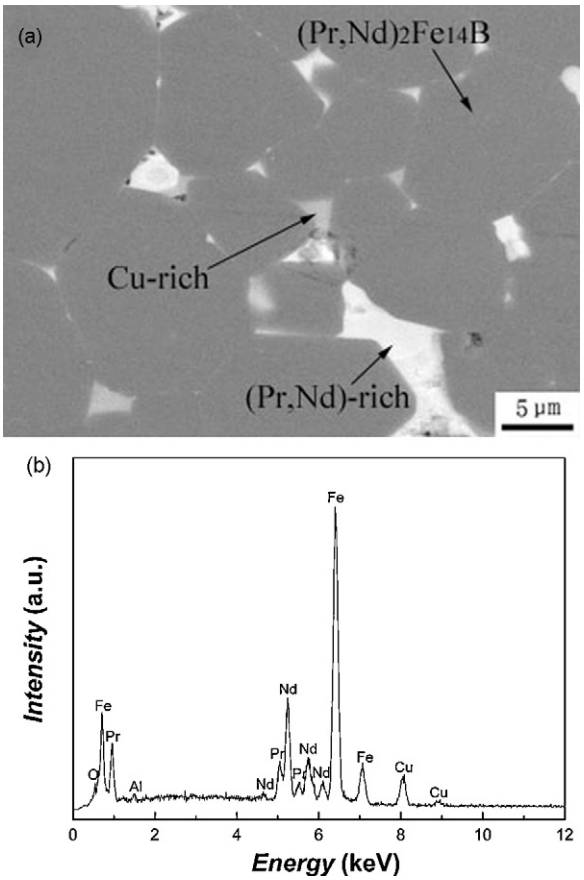

Fig. 3. (a) SEM back-scattered image of annealed magnet with 1.2 wt% $Al_{85}Cu_{15}$ addition, and (b) EDX spectrum of the Cu-rich phase marked in (a).

Table 1
Open-circuit potentials of alloys measured in Ar-purged 0.049% H_2SO_4 and 3.5% NaCl solutions with respect to a saturated calomel electrode.

Alloy	Potential (V)	
	0.049% H_2SO_4	3.5% NaCl
(Pr, Nd)$_{22}$Fe$_{56}$Cu$_{10}$Al$_2$O$_{10}$	−0.784	−0.735
(Pr, Nd)$_{11.76}$Fe$_{82.36}$B$_{5.88}$	−0.707	−0.700
(Pr, Nd)$_{80}$Fe$_{20}$	−0.870	−1.191

phase) and (Pr, Nd)$_{11.76}$Fe$_{82.36}$B$_{5.88}$ ((Pr, Nd)$_2$Fe$_{14}$B phase) were respectively prepared through vacuum induction melting. Their open-circuit potentials were measured with reference to a saturated calomel electrode in 0.049% H_2SO_4 and 3.5% NaCl solutions and listed in Table 1. Their mass loss in humid atmosphere was also measured and shown in Fig. 4. The open-circuit potentials of Cu-rich and (Pr, Nd)$_2$Fe$_{14}$B phases are far higher than that of the (Pr, Nd)-rich phase. This indicates that the thermodynamic stability of Cu-rich phase is higher than that of the (Pr, Nd)-rich phase. Moreover, the Cu-rich and (Pr, Nd)$_2$Fe$_{14}$B phases hardly have mass loss after exposed for 96 h at 120 °C, 2 bar and 100% relative humidity atmosphere. However, after exposed in humid environments for only 24 h the mass loss of the (Pr, Nd)-rich phase reaches 256.8 mg/cm^2, which is mostly based on the falling out of whole grains by oxidation.

From the EDX results, as $Al_{85}Cu_{15}$ was added, Cu and Al dissolve into the intergranular regions to form a Al- and Cu-containing more stable (Pr, Nd)-rich phase, which replaces the pure (Pr, Nd)-rich phase. Coupled with the occurrence of Cu-rich phase, the grain boundary microstructure is changed by segregation of Al and Cu. It inhibits the corrosion of the intergranular phase in saline and weak acidic electrolytes. Moreover, higher additions of $Al_{85}Cu_{15}$ may increase the corrosion inhibition. Thus, with the increase of $Al_{85}Cu_{15}$ addition amount from 0 to 1.2 wt%, the polarization current density is reduced under the same applied potential at the anodic branch of the polarization cures (Fig. 1a and b) and i_{corr} gets lower (Fig. 1c and d). As shown in Fig. 4, it can be revealed that the (Pr, Nd)$_2$Fe$_{14}$B phase hardly reacts with water, while the (Pr, Nd)-rich phase significantly reacts with water. This indicates that the mass loss of magnets in humid environments is strongly related to the corrosion of the (Pr, Nd)-rich intergranular phase, which is controlled by its thermodynamic stability [9,17]. For the $Al_{85}Cu_{15}$-free magnet, the (Pr, Nd)-rich intergranular phase is active and the driving force for corrosion reactions of the (Pr, Nd)-rich phase with water is high. The $Al_{85}Cu_{15}$-free magnet is thus susceptible to corrosion in humid environments, as is evident in Fig. 2. For the $Al_{85}Cu_{15}$-added magnets, especially magnet with 1.2 wt% $Al_{85}Cu_{15}$,

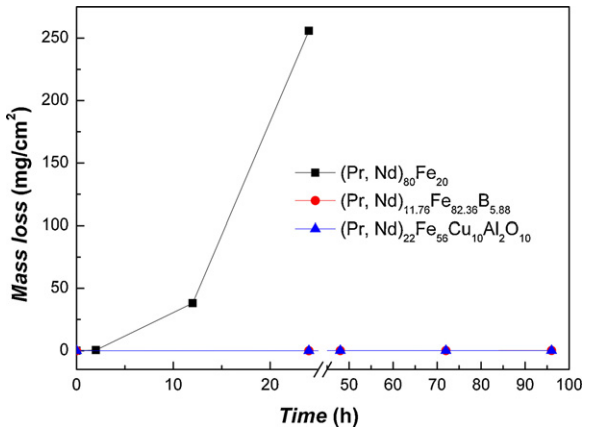

Fig. 4. Mass loss of (Pr, Nd)$_{22}$Fe$_{56}$Cu$_{10}$Al$_2$O$_{10}$, (Pr, Nd)$_{11.76}$Fe$_{82.36}$B$_{5.88}$ and (Pr, Nd)$_{80}$Fe$_{20}$ measured in 120 °C, 2 bar and 100% relative humidity atmosphere for different times.

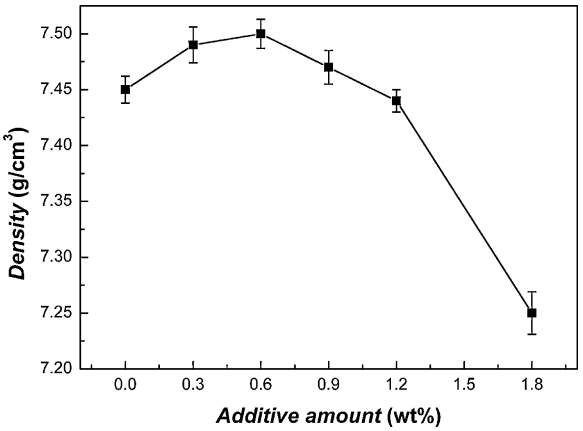

Fig. 5. Magnet density as a function of $Al_{85}Cu_{15}$ addition amount. The error bar represents the standard deviation obtained from 5 samples.

the stability enhancement of intergranular phase by dissolutions of Al and Cu decreases the driving force for the intergranular corrosion, thus decreasing the mass loss. Additionally, the formation of Cu-rich phase means a diminution of the (Pr, Nd)-rich grain boundary fraction, which also decreases the mass loss of magnets because the Cu-rich phase hardly reacts with water. Consequently, the $Al_{85}Cu_{15}$-added magnets in humid environments are far more stable than the $Al_{85}Cu_{15}$-free magnet.

The corrosion resistance of Nd–Fe–B sintered magnets is also related to the magnet density [19]. Fig. 5 shows the magnet density as a function of $Al_{85}Cu_{15}$ addition amount. With increasing the $Al_{85}Cu_{15}$ amount from 0 to 0.6 wt%, the magnet density increases, which is beneficial to improve the corrosion resistance. Over 0.6 wt%, the magnet density tends to fall. But the corrosion resistance of magnets is still improved, as shown in Figs. 1 and 2. It

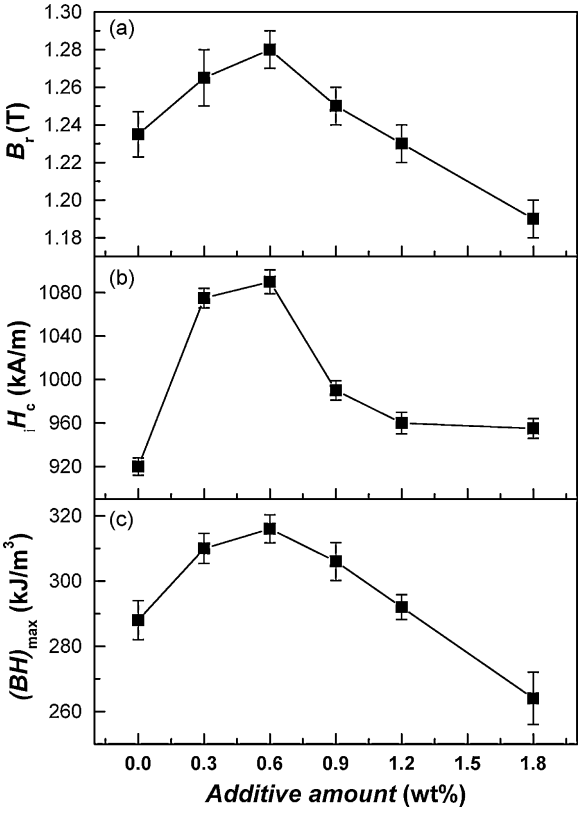

Fig. 6. Magnetic properties of the magnets as a function of $Al_{85}Cu_{15}$ addition amount. The error bar represents the standard deviation obtained from 5 samples.

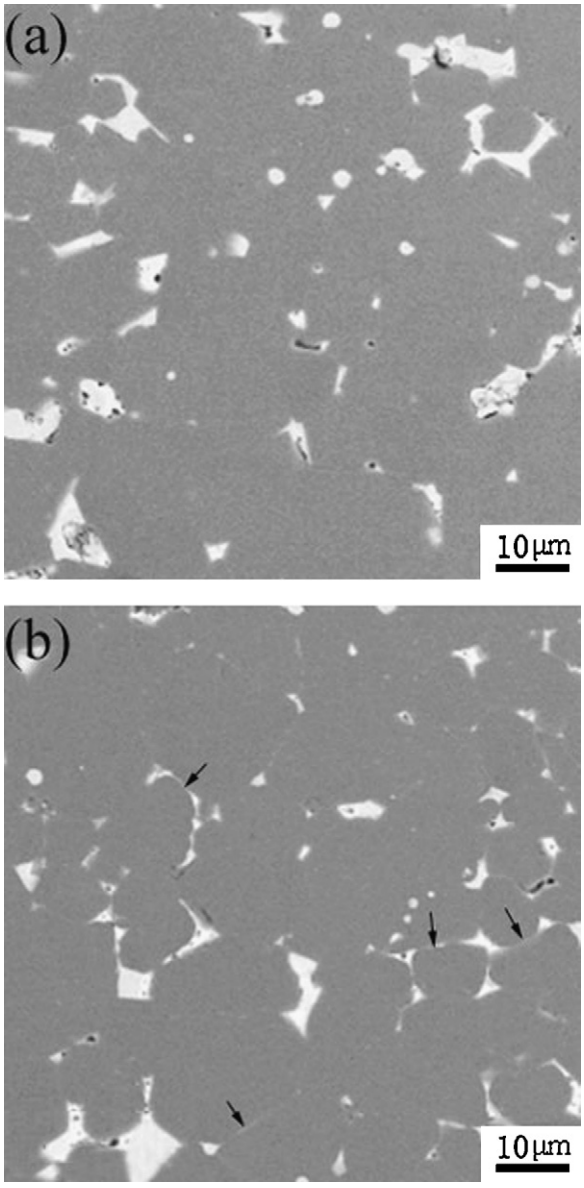

Fig. 7. SEM back-scattered images of Nd–Fe–B magnets with (a) 0 wt% and (b) 0.6 wt% $Al_{85}Cu_{15}$ addition.

indicates that the stability enhancement of the (Pr, Nd)-rich intergranular phase and the occurrence of the Cu-rich phase overshadow the magnet density effect on the corrosion resistance.

3.2. Magnetic properties

Fig. 6 shows the effect of $Al_{85}Cu_{15}$ intergranular addition on the magnetic properties of $(Pr, Nd)_{14.8}Fe_{78.7}B_{6.5}$. Remanence B_r, coercivity $_iH_c$ and maximum energy product $(BH)_{max}$ all initially increase considerably up to 0.6 wt%, and sequentially decrease with the further increase of $Al_{85}Cu_{15}$ addition amount. The peak values of $_iH_c$ and $(BH)_{max}$, 1090 kA/m and 316 kJ/m^3 are all obtained at the 0.6 wt% $Al_{85}Cu_{15}$, enhanced by approximately 18% and 10%, respectively in comparison with the $Al_{85}Cu_{15}$-free magnet.

The magnetic properties, especially B_r, are related to the magnet density as shown in Figs. 5 and 6. In addition, the magnetic properties, especially $_iH_c$, are also related to the microstructural modification of magnets. Fig. 7 shows the SEM back-scattered images of magnets with 0 and 0.6 wt% $Al_{85}Cu_{15}$. In Fig. 7a, for the $Al_{85}Cu_{15}$-free magnet, the (Pr, Nd)-rich phase agglomerates at

the triple junctions. It is difficult to see the distribution of the (Pr, Nd)-rich phase around the $(Pr, Nd)_2Fe_{14}B$ grains. In Fig. 7b, for the magnet with 0.6 wt% $Al_{85}Cu_{15}$, the volume fraction of the (Pr, Nd)-rich phase at the triple junctions decreases. A larger amount of (Pr, Nd)-rich phase distributes around the $(Pr, Nd)_2Fe_{14}B$ grains (indicated by arrows). The $(Pr, Nd)_2Fe_{14}B$ grains of the magnet with 0.6 wt% $Al_{85}Cu_{15}$ are well isolated, which improves the magnetic decoupling thus enhancing ${}_iH_c$. Moreover, the homogeneous distribution of (Pr, Nd)-rich phase can reduce the stray demagnetizing fields, which decreases the nucleation of reverse magnetic domains thereby increasing ${}_iH_c$. Consequently, the improvement of magnetic properties is related to the microstructural modification and the increase of magnet density.

4. Conclusions

(1) Corrosion resistance of $(Pr, Nd)_{14.8}Fe_{78.7}B_{6.5}$ magnets is remarkably improved by $Al_{85}Cu_{15}$ intergranular addition. It can be ascribed to the stability enhancement of (Pr, Nd)-rich intergranular phase and the formation of Cu-rich phase.
(2) Magnetic properties of $(Pr, Nd)_{14.8}Fe_{78.7}B_{6.5}$ magnets are also enhanced by $Al_{85}Cu_{15}$ intergranular addition. Optimum magnetic properties are obtained at the addition amount of 0.6 wt%. This is related to the microstructural modification and the increase of magnet density.

Acknowledgments

This work was supported by the National Natural Science Foundation of China (NSFC-50971113), 863 program of China (No: 2009AA03Z112) and IRT-0651.

References

[1] W.J. Mo, L.T. Zhang, A.D. Shan, L.J. Cao, J.S. Wu, M. Komuro, J. Alloys Compd. 461 (2008) 351–354.
[2] G. Yan, P.J. McGuiness, J.P.G. Farr, I.R. Harris, J. Alloys Compd. 478 (2009) 188–192.
[3] X.G. Cui, M. Yan, T.Y. Ma, W. Luo, S.J. Tu, J. Magn. Magn. Mater. 321 (2009) 392–395.
[4] A.A. El-Moneim, A. Gebert, F. Schneider, O. Gutfleisch, L. Schultz, Corros. Sci. 44 (2002) 1097–1112.
[5] W.Q. Liu, M. Yue, D.T. Zhang, J.X. Zhang, X.B. Liu, J. Appl. Phys. 105 (2009) 07A709-1-3.
[6] N.D. Tomashov, G.P. Chernova, Corrosion and Corrosion-resistant Alloys, Chemical Industry Press, China, 1982, p. 137.
[7] W.C. Wu, H.Q. Feng, K.Z. Wu, Tables of Standard Electrode Potentials, Science Press, China, 1991, p. 25.
[8] X.G. Cui, M. Yan, T.Y. Ma, L.Q. Yu, Physica B 403 (2008) 4182–4185.
[9] M. Katter, L. Zapf, R. Blank, W. Fernengel, W. Rodewald, IEEE Trans. Magn. 37 (2001) 2474–2476.
[10] J.P. Nozieres, D.W. Taylor, H. Bala, M. Malik, S. Szymura, H. Stoklosa, J. Alloys Compd. 186 (1994) 201–208.
[11] S. Szymura, H. Bala, H. Stoklosa, V.V. Sergeev, Phys. Stat. Sol. (a) 137 (1993) 179–188.
[12] O. Filip, A.M. El-Aziz, R. Hermann, K. Mummert, L. Schultz, Mater. Lett. 51 (2001) 213–218.
[13] H. Bala, S. Szymura, E. Owczarek, W.N. Wiechula, Intermetallics 5 (1997) 493–495.
[14] S. Pandian, V. Chandrasekaran, G. Markandeyulu, K.J.L. Iyer, K.V.S. Rama Rao, J. Appl. Phys. 92 (2002) 6082–6086.
[15] A.R. Yan, X.P. Song, X.T. Wang, J. Magn. Magn. Mater. 169 (1997) 193–198.
[16] L.Q. Yu, Y.H. Wen, M. Yan, J. Magn. Magn. Mater. 283 (2004) 353–356.
[17] D.F. Cygan, M.J. Mcnallan, J. Magn. Magn. Mater. 139 (1995) 131–138.
[18] S.Z. Zhou, Q.F. Dong, Supermagnets: Rare-earth & Iron System Permanent Magnet, Metallurgical Industry Press, China, 1999, p. 263.
[19] G. Yan, A.J. Williams, J.P.G. Farr, I.R. Harris, J. Alloys Compd. 292 (1999) 266–274.